

International Conference on Manufacture of Lightweight Components – ManuLight2014

Effect of Solubilisation on the High-Temperature Formability of AA6016 Sheets

P.F. Bariani¹, S. Bruschi^{1*}, A. Ghiotti¹, F. Michieletto¹

¹ Department of Industrial Engineering, University of Padova, Italy

* Corresponding author. Tel.: +39 (0) 49 8276821; fax: +39 (0) 49 8276816 E-mail address: stefania.bruschi@unipd.it

Abstract

The paper investigates the formability behaviour and post-forming characteristics of AA6016 sheets in a range of temperatures and strain rates typical of hot stamping. Since the as-delivered condition of the blanks was the T4 treatment, the blanks were subjected to two different thermal cycles before testing: one implying the material solubilisation and subsequent cooling and deformation at the testing temperature, and the other without any solubilisation. The influence of the solubilisation on the material flow stress, true strain at fracture, and post-forming mechanical and surface characteristics is highlighted. The optimal combination of process parameters assuring the best formability and surface characteristics is identified, validating the results through hot stamping trials carried out on a real component.

© 2014 Elsevier B.V. This is an open access article under the CC BY-NC-ND license (<http://creativecommons.org/licenses/by-nc-nd/3.0/>).

Peer-review under responsibility of the International Scientific Committee of the “International Conference on Manufacture of Lightweight Components – ManuLight 2014”

Keywords: Hot Stamping; Aluminum Alloy; Solubilisation.

1. Introduction

In recent years, the forming of high strength aluminium alloys sheets at elevated temperature has gained a renewed interest for the manufacture of parts of the car body-in-white and chassis on the basis of the more and more stringent requirements in terms of weight and fuel consumption reduction on one hand, and increase of passengers' safety on the other. Being these alloys usually characterized by reduced formability when formed at room temperature, a number of scientific studies are now focusing on different means to enhance their formability limits [1]. One possibility is represented by the hot stamping process, during which the blank is heated at elevated temperature and simultaneously formed and quenched inside cooled dies [2-4]. The authors recently investigated the behaviour of AA5083 sheets characterized by a conventional microstructure under temperature and strain rate conditions typical of the hot stamping process, and proved that complex-shaped parts can be formed if a well-defined formability window is respected [5].

In this paper, the behaviour of the aluminium alloy AA6016 delivered in the T4 condition is investigated under the same processing conditions applied in [5]. The AA6016 T4 presents an optimal corrosion resistance, good mechanical properties, and acceptable formability when formed at room temperature. AA6016 T4 sheets can be then cold formed to a certain extent, but the reduced strain at fracture presented by the alloy at room temperature prevents the production of more complex-shaped products. In order to overcome this drawback, the blank can be heated in the hot deformation temperature range to provide a significant enhancement of its formability [6-7]. Additionally, if the blank is heated up above its solubilisation temperature, which enables the dissolution of the precipitates within the aluminium matrix [8], a further enhancement in the formability should be envisaged, as in [9], where AA6082 alloy sheets were stamped above the alloy solubilisation temperature proving a significant increase in formability. On the other hand, the solubilisation lowers the as-delivered mechanical properties, and therefore may force a subsequent heat treatment on the

formed product to guarantee the required strength [10–11], and can affect the surface characteristics of the alloy. In the paper, the effect of the temperature and strain rate on the material formability in terms of strain at fracture and post-deformation characteristics is investigated by subjecting the as-delivered blanks to two different thermo-mechanical cycles, namely the material solubilisation and subsequent cooling and deformation at the testing temperature on one hand, and deformation at the testing temperature without any solubilisation on the other. The aim of this analysis is evaluate if the solubilisation treatment can affect the alloy behaviour during and after the hot stamping process. High temperature tensile tests were carried out to evaluate the material flow stress and strain at fracture, whereas the hardness and surface topography of the strained samples were measured to evaluate the material post-deformation characteristics. Industrial trials in a hot stamping plant were carried out on AA6016 alloy sheets subjected to the heat treatments in order to prove the obtained results.

2. Material

The chemical composition of the as-delivered AA6016 T4 is reported in Table 1.

Table 1. Chemical composition of the AA6016 T4 in the as-delivered condition (weight %).

Element	Si	Mg	Fe	Mn	Al
Weight [%]	4.28	0.69	0.16	0.06	Residual

The material is provided in sheets of 1.5 mm thickness. The material microstructure was analysed in the as-delivered condition and after being heat treated above its solubilisation temperature (equal to 550 °C) for five minutes, which represent the time required to dissolve the Mg₂Si precipitates within the aluminium matrix. After the solubilisation, the sheet samples were water-quenched to preserve their microstructure and readily observed to avoid natural ageing. The samples were mechanically polished and chemically etched by means of the Graff & Sargent etchant (84ml of H₂O, 15.5ml of HNO₃, 0.5 ml of HF and 3g CrO₃), in immersion for 10–15 minutes to evidence the grains. Fig. 1 shows the AA6016 microstructure in the as-delivered condition and after solubilisation: in both cases, the average grain size is between 50 and 55 µm, without any appreciable grain coarsening due to the thermal cycle. The SEM images of Fig. 2 show that the thermal cycle was effective in dissolving the Mg₂Si precipitates [12].

3. Experimental procedure

The tensile tests at elevated temperatures were carried

out on a MTS[®] hydraulic testing machine with a maximum load of 50 kN, equipped with an electromagnetic inductor heater able to heat the samples to the testing temperatures in a few seconds, and an air cooling equipment system to guarantee the desired cooling rate to the testing temperature.

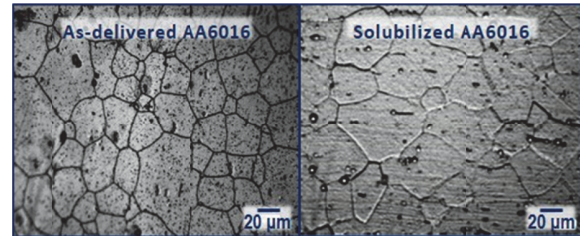


Fig. 1. AA6016 T4 microstructure in the as-delivered condition (left), and after solubilisation (right).

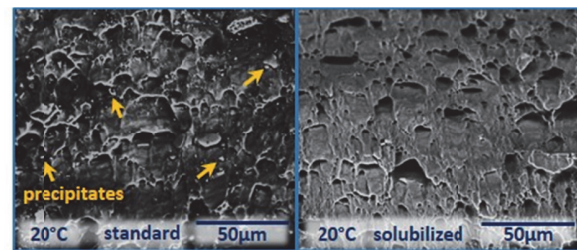


Fig. 2. SEM micrographs showing the presence (left) and absence (right) of the Mg₂Si precipitates within the aluminium matrix before and after solubilisation.

To measure in-line the sample deformation during the test and therefore calculate the material true strain, the optical measurement system Aramis[®] from GOM was utilized. During the tensile test, the sample temperature is controlled by means of a K-type thermocouple spot-welded in the centre of the gauge length, assuring an accuracy in the temperature measurement of ±1 °C. The overall tensile testing set-up is shown in Fig. 3.

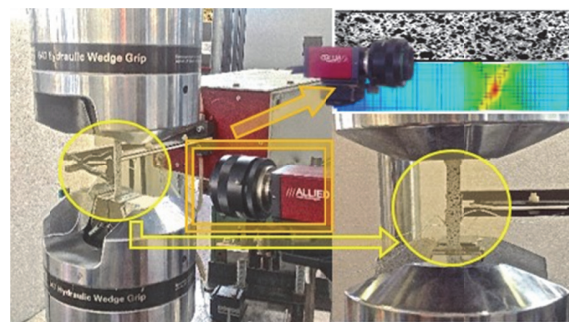


Fig. 3. Experimental apparatus for tensile tests at elevated temperature, composed by a MTS[®] multi-purpose press, an electromagnetic inductor heater, an air-cooling equipment, and the Aramis[®] optical measurement system from GOM[®].

The experimental plan for the tensile tests is shown in Table 2: 4 temperatures (besides the room temperature)

and 3 strain rates, kept constant during the test, were investigated for both the solubilized and not-solubilized sheets.

Table 2. Experimental plan for the tensile tests at elevated temperature.

Strain rate [s^{-1}]	Temperature [$^{\circ}C$]				Material condition
10^0	300	400	450	500	Non-solubilized
10^{-1}	300	400	450	500	&
10^{-2}	300	400	450	500	solubilized

Fig. 4 shows the temperature vs. time diagram of the tensile tests. The red line refers to a test without solubilisation, where the sample is heated up to the target temperature (always lower than the solubilisation temperature) with a heating rate of $12^{\circ}C/s$, than a soaking time of 90 s is applied for homogeneatization, and finally the material is tensile tested till fracture at constant temperature and strain rate. The blue line refers to a test where the sample is previously subjected to solubilisation at $550^{\circ}C$ for 5 minutes, then cooled down at $5^{\circ}C/s$ to the target temperature where it is strained till fracture, without any further soaking.

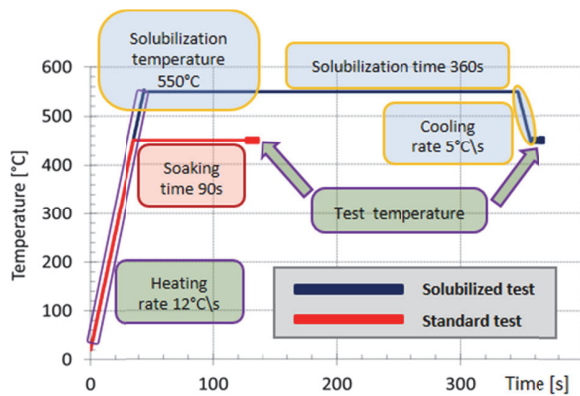


Fig. 4. Temperature vs. time diagram of the hot tensile tests. The red line refers to the standard tensile test and the blue line to the tensile test after solubilisation.

4. Flow behaviour and formability

Fig. 5 shows the flow stress sensitivity to temperature at a strain rate equal to $0.1s^{-1}$ for both the solubilized and non-solubilised material. Independently from its microstructural condition, the material exhibits a significant sensitivity to temperature and a reduced strain hardening at increasing temperature. Moreover, the solubilized material shows a lower flow stress compared to the not-solubilized one for each testing condition, being the difference more significant at decreasing temperature. The material flow stress

sensitivity to strain rate is instead shown in Fig. 6 at a temperature equal to $450^{\circ}C$: as expected, the material is strongly influenced by the strain rate. Furthermore, for the two lowest values of the strain rate, the flow stress of the not-solubilized material is higher than the solubilized one, whereas at $1s^{-1}$ the two are comparable. The same happens at $400^{\circ}C$ and $500^{\circ}C$, whereas at $300^{\circ}C$, the flow stress of the solubilized material is not influenced by the strain rate. It is worth to notice that the all the flow curves have been cut at a value of strain equal to 0.25, regardless to the actual strain at fracture, in order to provide a clearer view.

The true strain at fracture ϵ_f , considered as a measure of the material formability, was evaluated on the basis of the sample initial area by measuring its area at fracture according to eq. (1):

$$\epsilon_f = \ln \frac{A_{initial}}{A_{fracture}} \quad (1)$$

The true strain at fracture was not directly calculated from the Aramis measurements, since the specimen pattern at elevated temperature and very close to the fracture point was too deteriorated to provide reliable results.

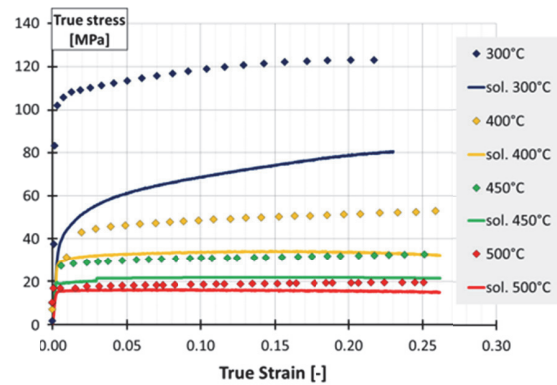


Fig. 5. True stress-true strain curves at varying temperature and strain rate equal to $0.1s^{-1}$. Solubilized condition (solid line) and not-solubilized condition (dotted line).

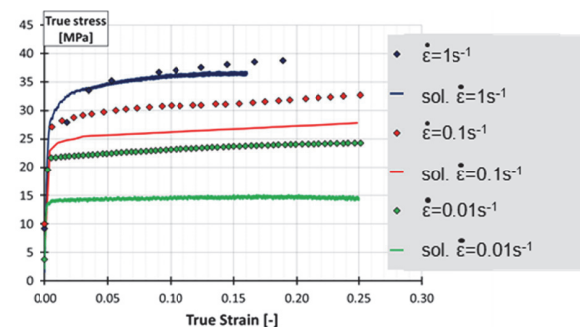


Fig. 6. True stress-true strain curves at varying strain rate and temperature equal to $450^{\circ}C$. Solubilized condition (solid line) and not-solubilized condition (dotted line).

Since the sample areas at fracture at the highest temperatures were very reduced, they were calculated measuring the width by means of a micrometre and the thickness by taking SEM micrographs to gain more accurate data (see Fig. 7).

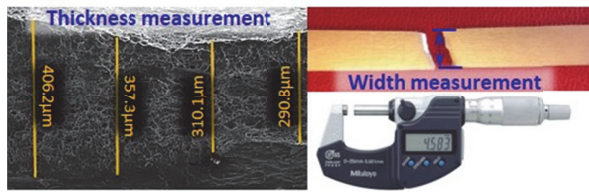


Fig. 7. Measurement approach for calculating the sample area at fracture.

The formability maps in terms of true strain at fracture as a function of the temperature and strain rate for the solubilized and the non-solubilised material are shown in Fig. 8 and 9, respectively.

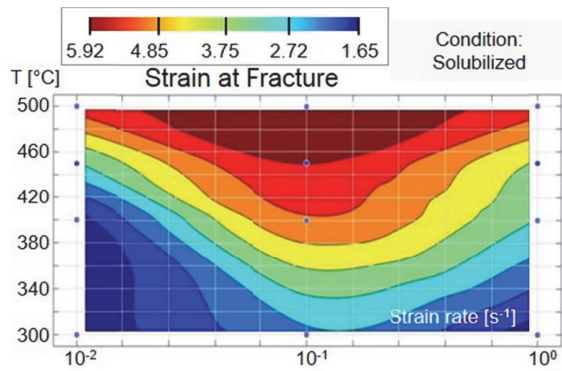


Fig. 8. Formability map of the solubilized material as a function of the temperature and strain rate.

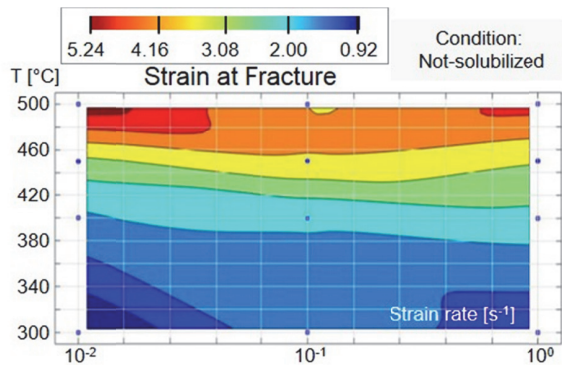


Fig. 9. Formability map of the not-solubilized material as a function of the temperature and strain rate.

The solubilized material shows a higher sensitivity to the strain rate, especially in the temperature intermediate range, with a wider formability window and highest values of formability shown for the temperatures of 450 °C and 500 °C. On the other hand, the not-solubilized material presents in general lower values of the true

strain at fracture, with a formability peak between 450 °C and 500 °C for the lowest and highest values of the strain rate.

The values of strain at UTS, representative of the necking onset, and therefore discriminating the uniform elongation in the sample from the non-uniform one, are reported in Fig. 10 as a function of the temperature and strain rate for the solubilized and the not-solubilized material. Except for the case of strain rate equal to 1 s⁻¹, the strain at UTS for the solubilized material is higher than the one of the not-solubilized material, implying a delay in the necking onset.

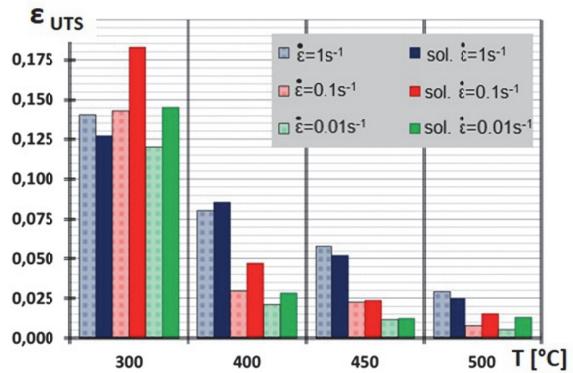


Fig. 10. True strain at UTS as a function of the temperature and strain rate. Solubilized condition (solid bar) and not-solubilized condition (dotted bar).

5. Post-deformation characteristics

The evaluation of the material post-deformation characteristics was carried out by means of micro-hardness measurements and surface roughness analysis nearby the sample fracture zone.

The Vickers micro-hardness was measured on the strained samples nearby the fracture zone and is shown in Fig. 11 as a function of the tensile testing temperature and strain rate for the solubilized and the non-solubilised material. As expected, the non-solubilised material shows higher hardness values, regardless to the testing condition, even if in general lower than the as-delivered material. In the temperature range of maximum formability, the not-solubilized material shows hardness values on an average 20% less than the one of the as-delivered blanks, but still acceptable. On the contrary, the hardness values of the solubilized material are drastically reduced, especially at 300 °C.

The surface topography of solubilized and not-solubilized samples after deformation was measured by means of a Sensofar Plu-Neox™ digital profilometer. Fig. 12 shows the results in the case of samples processed at 500 °C and 0.1 s⁻¹: it is evident that the solubilisation treatment greatly affects the surface

appearance and roughness. Whereas the not-solubilized sample presents a surface topography comparable to that of the as-delivered material, the solubilized sample has a surface that cannot be considered acceptable for the subsequent finishing operations.

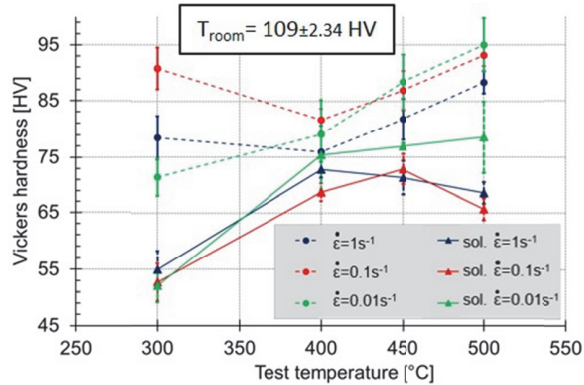


Fig. 11. Vickers micro-hardness after tensile testing as a function of the temperature and strain rate. Solubilized condition (solid line) and not-solubilized condition (dotted line).

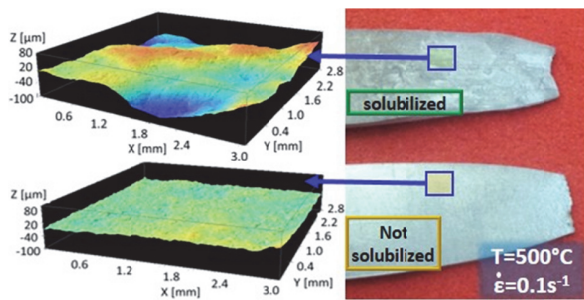


Fig. 12. Surface topography of solubilized and not-solubilized samples after deformation.

6. Industrial Trials

The same sheets of the laboratory tests were subjected to hot stamping trials to form an automotive component. The industrial plant consisted in a double effect hydraulic press and an external gas furnace for the blank heating. The dies were water cooled to guarantee a part rapid cooling after forming, while the mating surfaces of the dies were lubricated with oil.

Sheets subjected to both the heat treatments previously considered, namely solubilized and non-solubilized, were tested. In case of solubilized material, the initial blanks were kept in the furnace for 30 minutes at a temperature of 550°C to assure the complete dissolution of the precipitates. The stamping parameters were the same as found for the best forming condition from the laboratory test results: a temperature of 450°C and a

strain rate equal to 1 s⁻¹ on an average. The blank temperature when in contact with the dies was measured through an infrared thermocamera to acknowledge the average stamping temperature. Fig. 13 shows the different results obtained for the two heat-treated blanks: non-solubilized (A) and solubilized (B). As predicted by the laboratory tests, no failures were appreciable in the stamped parts, but a completely different surface appearance was shown even eye visible. Fig. 13 shows also that in both cases the stamped part microstructures is not affected by grain coarsening.

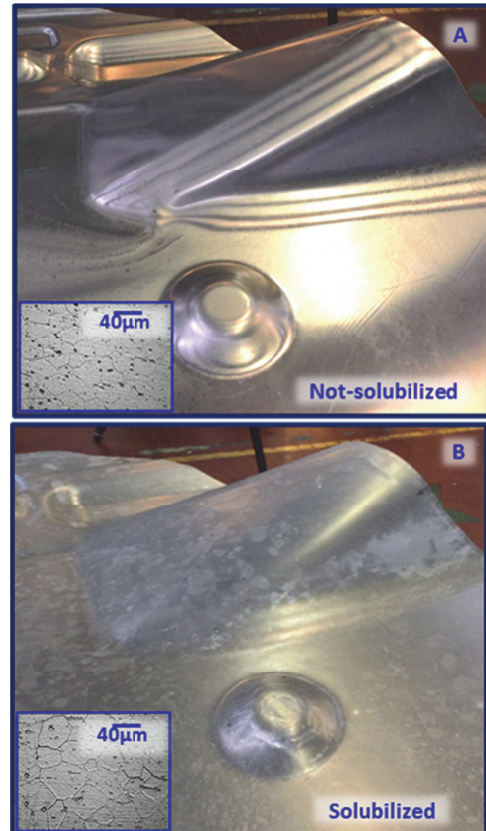


Fig. 13. Hot stamped part: non-solubilized condition (A), and solubilized condition (B).

7. Concluding remarks

Uni-axial tensile tests at elevated temperature were carried out on samples of AA6016 subjected to two different thermal cycles, one implying the solubilisation of the Mg₂Si precipitates and the other preserving the T4 condition of the as-delivered material. The material flow stress, true strain at fracture and at UTS, Vickers micro-hardness and surface topography after deformation were evaluated and compared. Furthermore, hot stamping trials on solubilized and not-solubilized sheets were carried out on an industrial plant for the production of an

automotive part by using the optimal process parameters identified in the laboratory tests. The following conclusions can be drawn:

- Both the solubilized and not-solubilized material flow stresses are highly sensible to temperature and strain rate in the investigated ranges.
- The solubilized material presents a wider formability window and higher true strain at fracture at 450 °C and 500 °C. The formability of the not-solubilized material is significantly higher at elevated temperature compared to that at room temperature.
- As expected, the Vickers micro-hardness of the solubilized samples after deformation is significantly lower than that of the as-delivered material. Whereas, the not-solubilized samples show still an acceptable hardness after deformation at the highest deformation temperatures.
- The solubilisation treatment greatly affects the surface topography of the samples after deformation, making unfeasible the subsequent finishing operations.
- Even if the solubilisation treatment can enhance the material formability to a significant extend, the obtainment of very rough surfaces after deformation, even eye visible, makes the solubilisation treatment unfeasible for hot stamping.
- The industrial trials confirm the results obtained from the laboratory tests. It is possible to use cold dies to shape aluminium alloy parts at elevated temperature and high strain rate, under hot stamping process conditions. The rough surface appearance of the solubilized parts after stamping proves that, even if the solubilisation heat treatment can improve the alloy formability, this kind of treatment cannot be used. On the other hand, the not-solubilized hot stamped parts present an optimal surface quality and respect very well the final shape without defects.

Acknowledgements

The Authors wish to thank the Italian Ministry of Economic Development for funding the Industry 2015 project “DefCom – Competitiveness in Deformation”, in the framework of which this research work was carried out.

References

- [1] Neugebauer, R.; Altan, T.; Geiger, M.; Kleiner, M.; Sterzing, A., 2006, Sheet metal forming at elevated temperatures. *CIRP Annals Manufacturing Technology*, Nr. 55/2, 2006, p. 799-816.
- [2] Karbasian, H.; Tekkaya, A.E., 2010. A review on hot stamping. *Journal of Materials Processing Technology*, Nr. 210, 2010, p. 2103-2118.
- [3] Bariani, P.F.; Bruschi, S.; Ghiotti, A.; Turetta, A., 2008. Testing formability in the hot stamping of HSS. *CIRP Annals Manufacturing Technology*, Nr. 57/1, 2008, p. 265–268.
- [4] Ghiotti, A.; Bruschi, S.; Borsetto, F., 2011, Tribological characteristics of high strength steel sheets under hot stamping conditions. *Journal of Materials Processing Technology*, Nr. 211/11, 2011, p. 1694-1700.
- [5] Bariani, P.F.; Bruschi, S.; Ghiotti, A.; Michieletto, F., 2013. Hot stamping of AA5083 aluminium alloy sheets. *CIRP Annals Manufacturing Technology*, Nr. 62, 2013, p. 251-254.
- [6] Toros, S.; Ozturk, F.; Kacar, I., 2008, Review of warm forming of aluminium-magnesium alloys. *Journal of Materials Processing Technology*, Nr. 207/1-3, 2008, p. 1-12.
- [7] Wang, L.; Strangwood, M.; Balint, D.S.; Lin, J.; Dean, T.A., 2010, Formability and failure mechanisms of 2024 under hot forming conditions. *Materials Science and Engineering: A*, Nr. 528/6, 2011, p. 2648-2656.
- [8] Garrett, R.P.; Lin, J.; Dean, T.A., 2005. An investigation of the effects of solution heat treatment on mechanical properties for AA6xxx alloys: experimentation and modelling. *International Journal of Plasticity*, Nr. 21/8, 2005, p. 1640-1657.
- [9] Mohamed, M.S.; Foster, A.D.; Lin, J.; Balint, D.S.; Dean, T.A., 2012, Investigation of deformation and failure features in hot stamping of AA6082: experimentation and modelling. *International Journal of Machine Tools and Manufacture*, Nr. 53/1, 2012, p. 27-38.
- [10] Olaf, E.; Jurgen, H., 2001, Texture control by thermomechanical processing of AA6xxx Al-Mg-Si sheet alloys for automotive applications (a review). *Material Science and Engineering*, 2001, Nr. A336, p. 249-262
- [11] Liu Hong, L.; Gang, Z.; Chun, L.; Liang, Z., 2006, Effects of different tempers on precipitation hardening of 6000 series aluminum alloys. *Transaction of Nonferrous Metals Society of China*, Nr. 17, 2006, p. 122-127.
- [12] Xiaobo, F.; Zhubin, H.; Shijian, Y.; Kailum, Z., 2013, Experimental investigation on hot forming-quenching integrated process of 6A02 aluminium alloy sheet. *Materials Science & Engineering A*, Nr. 573, 2013, p. 154-160.